J. Am. Chem. Soc. 1989, 111, 5733-5738

Synthesis, Interconversion, and Structural Characterization of the Closo and Nido Clusters $[(p\text{-Cymene})_3M_3S_2]^{2+}$ and $[(p\text{-Cymene})_3M_3S_2]^0$ (M = Ru, Os)

John R. Lockemeyer,[1] Thomas B. Rauchfuss,*[,1] and Arnold L. Rheingold*[,2]

Contribution from the School of Chemical Sciences, University of Illinois, Urbana, Illinois 61801, and Department of Chemistry, University of Delaware, Newark, Delaware 19711.

Received September 26, 1988

Abstract: The first (arene)metal sulfido clusters are described. Salts of the dicationic clusters of the general formula $[(p\text{-cymene})_3M_3S_2]^{2+}$ were prepared from the reaction of $[(p\text{-cymene})MCl_2]_2$ (M = Ru, $[\mathbf{1}]^{2+}$; M = Os, $[\mathbf{2}]^{2+}$) with $(Me_3Si)_2S$, methanolic NaSH, or aqueous Na_2S as sulfide sources. $[\mathbf{1}](PF_6)_2$ cyrstallizes in the triclinic space group $P\bar{1}$ with $a = 10.495$ (3) Å, $b = 11.064$ (3) Å, $c = 18.230$ (6) Å, $\alpha = 100.62$ (2)°, $\beta = 90.93$ (3)°, $\gamma = 115.40$ (2)°, $Z = 2$, and $d_{calcd} = 1.883$ g cm^{-3}. The dication $[\mathbf{1}]^{2+}$ exists as a closo trigonal-bipyramidal cluster with Ru–Ru distances of 2.763 (3)–2.796 (1) Å and an average Ru–S distance of 2.338 (2) Å. Cyclic voltammetric studies show that $[\mathbf{1}]^{2+}$ undergoes two one-electron reductions separated by only 0.137 V vs Ag/AgCl, and $[\mathbf{2}]^{2+}$ undergoes a *simultaneous* two-electron reduction at −0.761 V vs Ag/AgCl. Cobaltocene reduction of $[\mathbf{1}](PF_6)_2$ gives dark blue $[\mathbf{1}]^0$. This neutral Ru_3S_2 cluster crystallizes in the triclinic space group $P\bar{1}$ with $a = 9.958$ (3) Å, $b = 10.270$ (3) Å, $c = 15.338$ (5) Å, $\alpha = 78.26$ (2)°, $\beta = 85.92$ (3)°, $\gamma = 78.53$ (2)°, $Z = 2$, and $d_{calcd} = 1.700$ g cm^{-3}. $[\mathbf{1}]^0$ adopts a nido framework with two bonding Ru–Ru distances of 2.733 (1) and 2.712 (1) Å and a nonbonding Ru–Ru distance of 3.612 (1) Å. The average Ru–S distances are elongated with respect to the closo cluster. The cymene ligands are bound in an η^6-fashion and are closer to the metal centers by an average of 0.015 (6) Å. The reduced cluster is highly reactive, and it is oxidized by H^+ to regenerate the dicationic closo cluster.

The organometallic chemistry of metal sulfido clusters is dominated by their carbonyl derivatives. Homo- and heterometallic compounds are known, most of which have been prepared from the reactions of neutral or anionic carbonyls with elemental sulfur. The strong acceptor properties of CO ligands promote strong metal-metal bonding and often lead to the formation of anionic clusters. A large fraction of these derivatives are built up of $M(CO)_3$ vertices, and it is therefore appealing to consider related families of clusters with other ML_3 vertices. In view of the weak acceptor ability of arenes,[3] the corresponding $[M(\text{arene})]_xS_y$ species might be expected to exhibit unusual properties. Additionally, given the extensive use of arene complexes in organic synthesis, $[M(\text{arene})]_x$ clusters may lead to new synthetic opportunities which exploit the unique capabilities of multimetallic reaction centers.[4]

The first arene metal clusters were prepared by Fischer and Rörscheid and have the composition $M_3(\text{arene})_3Cl_6^+$, where M = Ti, Zr, Nb, and Ta.[5] These often mentioned clusters have received only occasional study since their structures were determined in 1974.[6] In 1975, Stephenson described the characterization of cuboidal $[Ru_4(OH)_4(\text{arene})_4]^{4+}$ formed by the base hydrolysis of $[(\text{benzene})RuCl_2]_2$.[7] The electron-deficient clusters $[M_4H_4(\text{arene})_4]^{2+}$ (M = Ru, Os) have been briefly reported.[8] While no M–S–arene clusters are known, the M–S–CO clusters continue to attract much attention.[9]

Results and Discussion

Background. Central to arene ruthenium chemistry are the dimeric $[(\text{arene})RuCl_2]_2$ prepared from the reaction of cyclohexadienes and hydrated ruthenium trichloride. The *p*-cymene (4-isopropyltoluene) derivative of these dimers was selected for this study because of its good solubility (vs the benzene and hexamethylbenzene derivatives), ease of synthesis from commercially available α-phellandrene, and the convenient ^1H NMR characteristics of its derivatives.

Synthesis of $[(p\text{-Cymene})_3M_3S_2]^{2+}$. Early in this project we found that the reaction of aqueous solutions of $Na_2S{\cdot}9H_2O$ and $[(p\text{-cymene})RuCl_2]_2$ resulted in an immediate color change to red-brown. Addition of excess KPF_6 to the filtered reaction mixture gave $[(\text{cymene})_3Ru_3S_2](PF_6)_2$ ($[\mathbf{1}](PF_6)_2$) in 44% recrystallized yield (eq 1). It was found that this reaction is sensitive to pH, with neutral to acidic conditions favoring the formation of the product.

$$^3/_2[(\text{cymene})RuCl_2]_2 + 2S^{2-} \rightarrow \underset{[\mathbf{1}]^{2+}}{[(\text{cymene})_3Ru_3S_2]^{2+}} + 6Cl^- \qquad (1)$$

Solutions buffered at pH 10 gave no color change upon addition of the sodium sulfide solution, possibly due to stability of hydroxo species. Salts of $[\mathbf{1}]^{2+}$ were also prepared in good yield from the reaction between $[(p\text{-cymene})RuCl_2]_2$ and NaSH in methanol. These results strongly suggest that $[\mathbf{1}]^{2+}$ forms via the reaction of SH^- in aqueous solution. A more efficient synthesis of $[(\text{cymene})_3Ru_3S_2]^{2+}$ involves the reaction between $(Me_3Si)_2S$[10] and $[(p\text{-cymene})RuCl_2]_2$ in THF. Metathesis of the resulting chocolate brown precipitate[11] with aqueous PF_6^- gave $[\mathbf{1}](PF_6)_2$.

Salts of $[\mathbf{1}]^{2+}$ are soluble in polar organic solvents, while the chloride and $O_3SCF_3^-$ derivatives are also water soluble. FAB mass spectrometry of $[\mathbf{1}](PF_6)_2$ supports the proposed formulation;

---

(1) University of Illinois.

(2) University of Delaware.

(3) Collman, J. P.; Hegedus, L. S.; Norton, J. R.; Finke, R. G. *Principles and Applications of Organotransition Metal Chemistry*; University of Science Books: Mill Valley, CA, **1987**; p 158.

(4) Gallop, M. A.; Johnson, B. F. G.; Lewis, J.; McCauley, A.; Perutz, R. N. *J. Chem. Soc., Chem. Commun.* **1988**, 1071.

(5) Fischer, E. O.; Rřscheid, F. *J. Organomet. Chem.* **1966**, *6*, 53.

(6) Churchill, M. R., Chang, S. W. Y. *J. Chem. Soc., Chem. Commun.* **1974**, 248. King, R. B.; Braitsch, D. M.; Kapoor, P. N. *J. Am. Chem. Soc.* **1975**, *97*, 60.

(7) Gould, R. O.; Jones, C. L.; Robertson, D. R.; Stephenson, T. A. *J. Chem. Soc., Chem. Commun.* **1977**, 222.

(8) Cabeza, J. A.; Nutton, A.; Mann, B. E.; Brevard, C.; Maitlis, P. M. *Inorg. Chim. Acta* **1986**, *115*, L47.

(9) For recent studies on Ru–S carbonyls, see, $Ru_8(CO)_{17}S_2(\text{toluene})$: Adams, R. D.; Babin, J. E.; Tasi, M. *Inorg. Chem.* **1986**, *25*, 4460. $(CpMo)_2RuS(CO)_7$: Adams, R. D.; Babin, J. E.; Tasi, M. *Organometallics* **1988**, *7*, 219.

(10) Recent applications of the $(Me_3Si)_2S$ and $(Me_3Si)_2Se$ methodology: Snyder, B. S.; Holm, R. H. *Inorg. Chem.* **1988**, *27*, 2339. Darkwa, J. D.; Lockemeyer, J. R.; Boyd, P. D. W.; Rauchfuss, T. B.; Rheingold, A. L. *J. Am. Chem. Soc.* **1988**, *110*, 141. Fenske, D.; Hollnagel, A.; Merzweiler, K. *Z. Naturforsch.* **1988**, *43B*, 634. Martin, M. J.; Qiang, G.-H.; Schleich, D. M. *Inorg. Chem.* **1988**, *27*, 2804. A review on the subject: Fenske, D.; Ohmer, J.; Hachgenai, J.; Merzweiler, K. *Angew. Chem., Int. Ed. Engl.* **1988**, *27*, 1277.

0002-7863/89/1511-5733$01.50/0

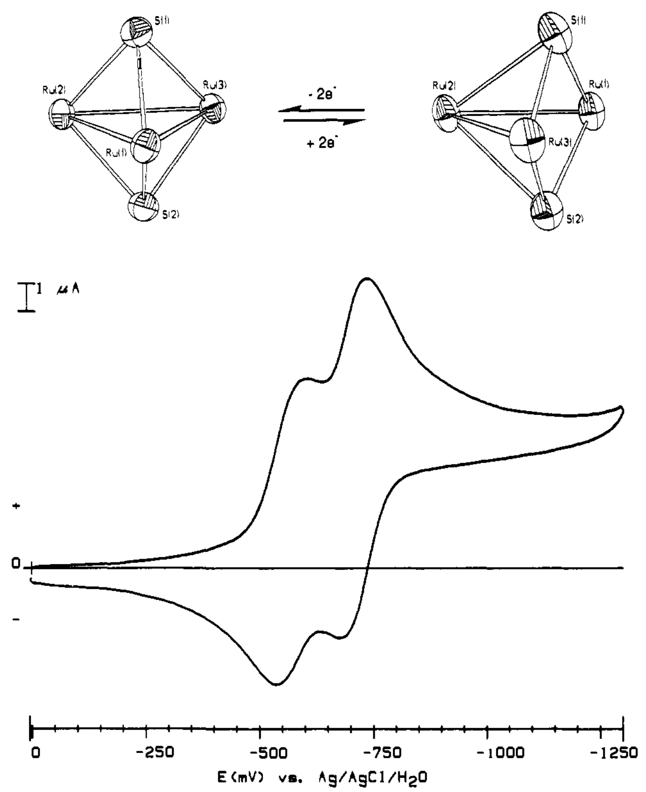

Figure 1. Cyclic voltammogram of $[\mathbf{1}](PF_6)_2$, 1.0 mM in CH_2Cl_2. The Ru_3S_2 core structures are shown for the electrochemically interrelated $[\mathbf{1}]^{2+}$ and $[\mathbf{1}]^0$. The scan rate is 0.100 V/s and the reference electrode is Ag/AgCl.

the $[(\text{cymene})_3Ru_3S_2]^+$ parent ion peak appears at $m/e = 771$ (^{102}Ru) with the expected isotopic distribution pattern. The new compounds exhibit simple 300 MHz ^1H NMR spectra, indicative of equivalent, symmetrical cymene groups.[11] Satisfactory elemental analyses were obtained for the PF_6^- and $O_3SCF_3^-$ salts of [**1**], but analyses for the supposed $[\mathbf{1}]Cl_2$ were variable. Conductivity measurements on CH_3NO_2 solutions of $[\mathbf{1}](PF_6)_2$ were indicative of a 2:1 electrolyte, having a molar conductivity of 179 ohm^{-1} cm^2 mol^{-1}.

Solutions of $[\mathbf{1}]^{2+}$ are remarkably stable. Aqueous solutions of the triflate salt were unaffected by boiling for 1 day. Attempts to displace the cymene ligands with other π-acid ligands such as CO (2 atm/25 °C), CH_3CN (reflux and/or UV irradiation), hexamethylbenzene (190 °C melt), and tetramethylthiophene (200 °C and/or UV irradiation) resulted only in recovery of starting materials.

Synthesis of $[(\text{cymene})_3Os_3S_2]^{2+}$ salts was accomplished via the silyl sulfide route from $[(p\text{-cymene})OsCl_2]_2$. The PF_6^- salt of this compound exists as red-orange, air-stable microcrystals. Its ^1H NMR spectrum closely resembles that for the ruthenium analogue, again indicating a closo structure.

Electrochemistry and Redox Reactions. Cyclic voltammetry established that $[\mathbf{1}]^{2+}$ undergoes two very closely spaced one-electron reductions centered at −0.567 and −0.704 V vs Ag/AgCl (Figure 1). On the basis of i_a/i_c ratios and ΔE_p values, the reductions are reversible.[12] Controlled potential electrolysis of stirred CH_3CN solutions of $[\mathbf{1}](PF_6)_2$ at −1500 mV consumes 1.98 Faraday, confirming the 2e nature of the reduction. As noted by Taube,[13] the $E_{1/2}$ separation in sequential redox processes can be used to calculate the comproportionation constant K_c. The calculation of the comproportionation constant for the formation of $[\mathbf{1}]^+$ from $[\mathbf{1}]^{2+}$ and [**1**], using eq 2, gave a value of 10.1. In eq 2, $E°_1$ and $E°_2$ were taken as $E_{1/2}$'s, $n_1 = n_2 = 1$, $F/RT = 0.0591$ V. For $\Delta E_{1/2} > 130$ mV, $E_{1/2} = (E_{pc} + E_{pa})/2$.

$$K_c = \exp[(E°_1 - E°_2)n_1n_2F/RT] = ([\mathbf{1}]^+)^2/([\mathbf{1}]^{2+})([\mathbf{1}]^0) \quad (2)$$

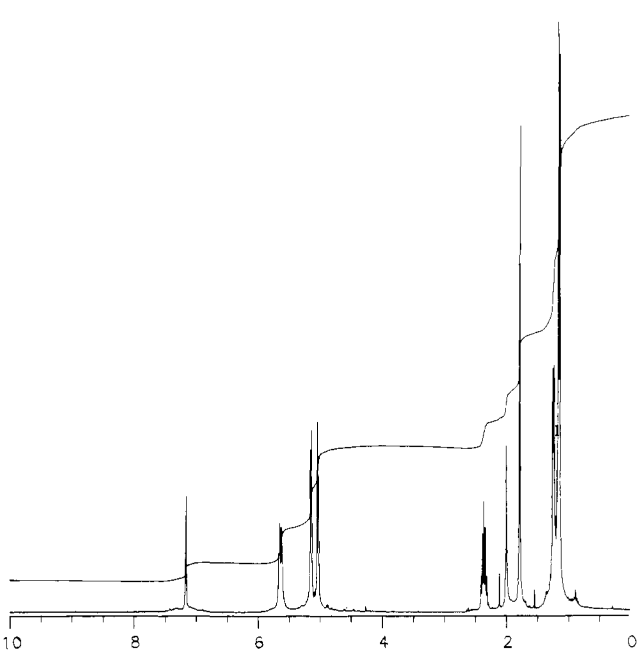

Figure 2. 300 MHz ^1H NMR spectrum of $[(p\text{-cymene})_3Ru_3S_2]$, $[\mathbf{1}]^0$ (C_6D_6 solution).

As suggested by electrochemical studies, the dication $[\mathbf{1}]^{2+}$ may be chemically reduced to the neutral form $[\mathbf{1}]^0$. Addition of an acetonitrile solution of $[\mathbf{1}](PF_6)_2$ to 2 equiv of Cp_2Co in CH_3CN gave $(\text{cymene})_3Ru_3S_2$ (eq 3). The deep blue neutral cluster can

$$\underset{[\mathbf{1}]^{2+}}{[(\text{cymene})_3Ru_3S_2]^{2+}} + 2Cp_2Co \rightarrow \underset{[\mathbf{1}]^0}{[(\text{cymene})_3Ru_3S_2]^0} + 2Cp_2Co^+ \quad (3)$$

be obtained in 92% yield following recrystallization from hexane at −78 °C. This cluster was assigned a nido structure based on its ^1H and ^{13}C NMR spectra, which reveal inequivalent cymene ligands in a 2:1 ratio (Figure 2).

Solutions of $(\text{cymene})_3Ru_3S_2$ are very reactive toward oxygen and moisture. Dichloromethane solutions of $[\mathbf{1}]^0$ (under N_2) are only stable for a few minutes at room temperature. As a solid, $[\mathbf{1}]^0$ is slowly oxidized by moist air.

An unusual illustration of the ability of $[\mathbf{1}]^0$ to serve as a 2e reductant is illustrated by its reaction with acids. Treatment of an ether solution of $[\mathbf{1}]^0$ with 1 equiv of $HOSO_2CF_3$ resulted in the precipitation of a 40% yield of $[\mathbf{1}](OTf)_2$. Failure of the mixture of solid $[\mathbf{1}]^{2+}$ and dissolved in $[\mathbf{1}]^0$ to comproportionate to $[\mathbf{1}]^+$ may be attributed to the poor solubility of $[\mathbf{1}](OTf)_2$ in Et_2O. The addition of a second equivalent of $HOSO_2CF_3$ to the deep blue filtrate resulted in a 34% yield of $[\mathbf{1}](OTf)_2$, leaving a nearly colorless filtrate. The precipitation of the closo cluster is accompanied by the evolution of a gas, presumably H_2. Mixing of equimolar *solutions* of the dicationic and neutral forms results in the formation of a red solution, which based on the aforementioned K_c calculations is mostly $[\mathbf{1}]^+$. Reaction of $[\mathbf{1}]^0$ with

---

(11) The chocolate-brown precipitate is thought to be primarily composed of $[\mathbf{1}]Cl_2$, but its ^1H NMR spectrum is distinct from that for the $(PF_6)_2$ salt, both in CD_2Cl_2. This difference may indicate (a) structurally distinct cluster cations or (b) ion pairing effects. The ^1H NMR spectra of D_2O solutions of "$[\mathbf{1}]Cl_2$" and the analytically pure $(OTf)_2$ salts are identical. $[(\text{cymene})_3Os_3S_2]Cl_2$ precipitates in purer form: Anal. Calcd for $C_{30}H_{42}Cl_2S_2Os_3$: C, 32.51; H, 3.82; Cl, 6.40; S, 5.78. Found: C, 33.04; H, 3.97; Cl, 6.38; S, 5.60. IR data on $[\mathbf{1}](PF_6)_2$ and $[\mathbf{1}](Cl)_2$ are identical except for bands due to the PF_6^- counterion.

(12) Geiger has described the electrochemistry of $Os_6(CO)_{18}^{0/2-}$, a 2e process that interconverts closo and "hypercloso" species. Tulyathan, B.; Geiger, W. E. *J. Am. Chem. Soc.* **1985**, *107*, 5960.

(13) Richardson, D. E.; Taube, H. *Inorg. Chem.* **1981**, *20*, 1278.

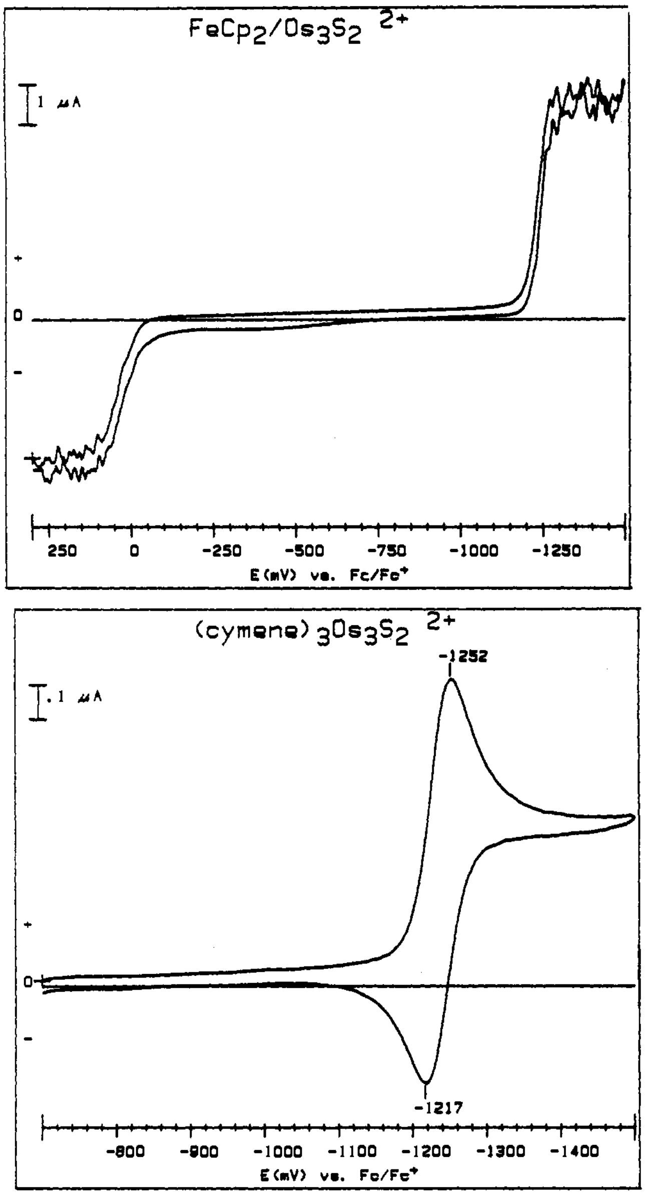

Figure 3. Bottom: cyclic voltammogram of $[\mathbf{2}](PF_6)_2$, 0.16 mM in CH_3CN. The scan rate is 10 mV/s. Top: cyclic voltammogram of a *stirred* mixture of $[\mathbf{2}](PF_6)_2$ and Cp_2Fe, 0.165 and 0.215 mM, respectively in CH_3CN. The scan rate is 50 mV/s. This hydrodynamic experiment supports the 2e stoichiometry. These voltammetry experiments are referenced to Cp_2Fe/Cp_2Fe^+.

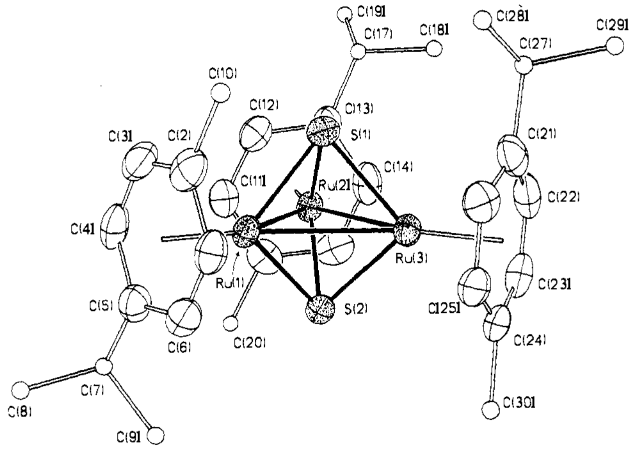

Figure 4. ORTEP drawing of the cationic portion of $[\mathbf{1}](PF_6)_2$ showing the labeling scheme for non-hydrogen atoms. Atoms comprising the Ru_3S_2 core are shaded for clarity.

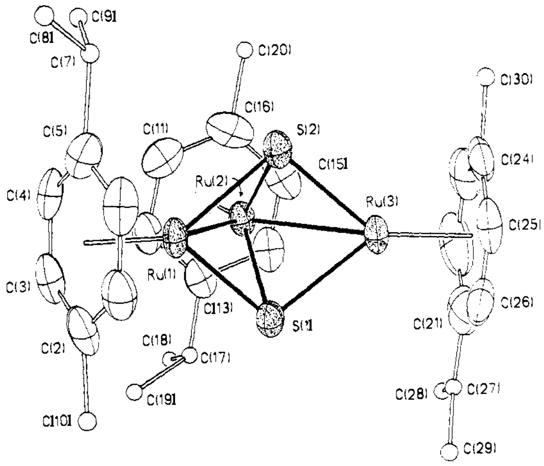

Figure 5. ORTEP drawing of $[\mathbf{1}]^0$ showing the atom labeling scheme for non-hydrogen atoms. Atoms comprising the Ru_3S_2 core are shaded for clarity.

Table I. Selected Bond Lengths (Å) and Angles (deg) for $[\mathbf{1}](PF_6)_2$ and $[\mathbf{1}]^0$

	$[\mathbf{1}](PF_6)_2$	$[\mathbf{1}]^0$
	Bond Lengths	
Ru(1)-Ru(2)	2.775 (1)	2.733 (1)
Ru(2)-Ru(3)	2.796 (1)	2.712 (1)
Ru(3)-Ru(1)	2.763 (1)	3.612 (1)
Ru(1)-S(1)	2.266 (2)	2.329 (2)
Ru(2)-S(1)	2.267 (2)	2.351 (2)
Ru(3)-S(1)	2.265 (1)	2.340 (2)
Ru(1)-S(2)	2.272 (1)	2.335 (2)
Ru(2)-S(2)	2.271 (2)	2.348 (2)
Ru(3)-S(2)	2.263 (2)	2.328 (2)
Ru(1)-CNT(1)	1.718 (6)	1.701 (8)
Ru(2)-CNT(2)	1.714 (7)	1.713 (7)
Ru(3)-CNT(3)	1.718 (6)	1.692 (9)
	Bond Angles	
Ru(1)-Ru(2)-Ru(3)	59.5 (1)	83.1 (1)
Ru(2)-Ru(3)-Ru(1)	59.9 (1)	
Ru(3)-Ru(1)-Ru(2)	60.6 (1)	
Ru(1)-S(1)-Ru(2)	75.5 (1)	71.5 (1)
Ru(1)-S(1)-Ru(3)	75.1 (5)	101.4 (1)
Ru(2)-S(1)-Ru(3)	76.2 (1)	70.6 (1)
Ru(1)-S(2)-Ru(2)	75.3 (1)	71.4 (1)
Ru(1)-S(2)-Ru(3)	75.1 (1)	101.6 (1)
Ru(2)-S(2)-Ru(3)	76.2 (1)	70.9 (1)
S(1)-Ru(1)-S(2)	89.9 (1)	77.7 (1)
S(1)-Ru(2)-S(2)	89.9 (1)	77.0 (1)
S(1)-Ru(3)-S(2)	90.1 (1)	77.6 (1)

$(cymene)Ru(CH_3CN)_3^{2+}$ did not lead to a tetranuclear $Ru_4S_2^{2+}$ complex but instead forms $[\mathbf{1}]^{2+}$.

The electrochemical properties of $[\mathbf{2}]^{2+}$ were also examined. The cyclic voltammogram in CH_2Cl_2 shows a single, nearly irreversible wave at −0.761 V, approximately 150 more cathodic than for the average of the two waves in $[\mathbf{1}]^{2+}$. The voltammogram of $[\mathbf{2}]^{2+}$ in CH_3CN at a slow scan rate provides a more reversible wave at −1.234 V vs Cp_2Fe/Cp_2Fe^+ (Figure 3). The 2e nature of this wave is indicated by comparison of i_c values with Cp_2Fe, resulting in a calculated 1.95e/mol $[\mathbf{2}]^{2+}$ (Figure 3). At a scan rate of 10 mV/s the ΔE_p value is 35 mV and $i_a/i_c = 0.91$. ΔE_p increases as the scan rate is increased. The reduction appears to be diffusion-controlled as indicated by the linearity of the plot of i_p vs $v^{1/2}$ over the range 50–1500 mV/s.

Crystallographic Studies on $[(Cymene)_3Ru_3S_2](PF_6)_2$ and $(Cymene)_3Ru_3S_2$. The structures of $[\mathbf{1}]^{2+}$ and $[\mathbf{1}]^0$ are shown in Figures 4 and 5, respectively. Pertinent bond lengths and angles are listed in Table I. The dication is comprised of a fairly regular trigonal-bipyramidal Ru_3S_2 core. Viewing the arenes as tridentate ligands, each ruthenium center in $[\mathbf{1}]^{2+}$ is seven coordinate. Each arene adopts a quite different orientation with respect to the Ru_3 plane. The average Ru–Ru distances of 2.778 (1) Å indicate single bonds. The average Ru–S distances are approximately 0.10 Å shorter than in neutral ruthenium sulfido carbonyls.[14]

The reduced species $[\mathbf{1}]^0$ consists of a square-pyramidal Ru_3S_2 core. The two Ru–Ru bonds are ca. 0.05 Å shorter than in $[\mathbf{1}]^{2+}$, while the long Ru···Ru contact is 3.612 (1) Å. Upon reduction of $[\mathbf{1}]^{2+}$ to $[\mathbf{1}]^0$ the average Ru–S distances increase by 0.071 (2) Å and the Ru–cymene (centroid) distances decrease by 0.015 Å.

Conclusions

Organometallic clusters of the general formula $[(cymene)_3M_3S_2]^{n+}$ (M = Os, n = 2; M = Ru, n = 2, 0) have been synthesized from the corresponding $[(cymene)MCl_2]_2$ and sulfide sources.[15] The syntheses result in the union of three $(cymene)Ru^{2+}$ units about a pair of triply bridging sulfido groups. The aqueous and methanolic syntheses are very likely mediated by SH^- since the pK_a of SH^- is 14.15,[16] at the limit of the aqueous range. Highly plausible intermediates would be analogues of $[(arene)Ru]_2(\mu\text{-}X_3)_2^+$ ($X = OH^-, Cl^-$).[17] The reaction of $(SiMe_3)_2S$ and $[(cymene)MCl_2]_2$ (M = Ru, Os) was expected to give $(arene)_4M_4S_4$, but again the closo dications are the only products obtained after metathesis in water.

The stability of $[\mathbf{1}]^{2+}$ may foreshadow an expanded family of cationic closo clusters of the type $[L_9Ru_3S_2]^{2+}$, with ligands L which are *not* strong π acceptors, e.g., H_2O, NH_3, and CH_3CN.

Our studies on $[(cymene)_3Ru_3S_2]^z$ provide an unprecedented example of the *electrochemical interconversion of closo and nido clusters wherein the end members have been structurally characterized*. Because of the weak acceptor properties of the arene ligands, the cluster cations are stablized. In contrast $M\text{–}S\text{–}(CO)_n$ clusters are rarely observed as cations, and the corresponding neutral $M_3S_2(CO)_9$ species are not appreciably reducing. We are unaware of other neutral metal clusters which are even nearly as reducing as $[\mathbf{1}]^0$.[18] The triosmium cluster is even more reducing than the ruthenium analogue.

The electrochemical properties of $[\mathbf{1}]^{2+}$ and $[\mathbf{2}]^{2+}$ are unusual. The redox potentials for two one-electron processes are usually well separated. For example in the related $Cp_3Co_3S_2$ (Cp = $C_5H_5^-$) system the two couples are separated by 0.46 V.[19,20] Examples of reversible two-electron redox processes are becoming increasingly common for di- and polymetallic assemblies.[12,18,21] In the present case, the basis of this unusual behavior is made clear by the crystallographic results: two-electron reduction of $[\mathbf{1}]^{2+}$ cleaves one Ru–Ru bond. It follows therefore that one-electron reduction would lead to partial metal–metal bond cleavage. Apparently the bond weakening that occurs upon partial reduction compensates for the diminished electrostatic driving force for the subsequent reduction. This effect is particularly pronounced in the case of $[(cymene)_3Os_3S_2]^{2+}$, which undergoes a two-electron reduction centered at −0.780 V vs Ag/AgCl. As discussed by Geiger,[12] *simultaneous* two-electron processes are unlikely; the results on $[\mathbf{1}]^{2+}$ and several related systems indicate that the second reduction is more favorable, or almost so, than the first. Apparently bi- and multimetallic arrays wherein the metals are constrained from complete dissociation are good candidates for the condition that $(E_1 - E_2) < 0$. A second example of this effect is provided by $(MeCp)_4Ru_4E_4^{2+/0}$, in the case of E = Se a single broadened wave is observed.[18] Interestingly $(C_5Me_5)_4Rh_4S_4$ exhibits two isolated one-electron waves.[22] Bedard and Dahl have reported at length on the redox properties of $Cp_3Co_3XY^z$ clusters which also undergo a single-wave two-electron redox process, but the dications could not be isolated in pure form.[23]

Table II. Crystal and Data Collection, Refinement Parameters for $[\mathbf{1}](PF_6)_2$ and $[\mathbf{1}]^0$

	$[\mathbf{1}](PF_6)_2$	$[\mathbf{1}]^0$
formula	$C_{30}H_{42}F_{12}P_2Ru_3S_2$	$C_{30}H_{42}Ru_3S_2$
lattice type	triclinic	triclinic
space group	$P\bar{1}$	$P\bar{1}$
a, Å	10.495 (3)	9.958 (3)
b, Å	11.064 (3)	10.270 (3)
c, Å	18.230 (6)	15.338 (5)
α, deg	100.62 (2)	78.26 (2)
β, deg	90.93 (3)	85.92 (3)
γ, deg	115.40 (2)	78.53 (2)
V, Å^3	1869 (1)	1504.3 (8)
Z	2	2
d_{calcd}, g cm^{-3}	1.883	1.700
μ, cm^{-1}	14.5	16.11
cryst dimen, mm	0.07 × 0.25 × 0.42	0.35 × 0.30 × 0.40
collection temp, °C	23	23
radiation type	Mo Kα (λ = 0.71073)	Mo Kα (λ = 0.71073)
2θ range, deg	4–50	4–52
read	6828	6135
unique	6591	5903
unique obsd	$4881 \geq 5\sigma(F_o)$	$4705 \geq 5\sigma(F_o)$
R_{int}, %	2.94	3.08
R_F, %	3.99	5.34
wR_F, %	4.39	5.86
GOF	1.156	1.394
data/parameter	11.0	14.9
$\Delta\rho$ max, e Å^{-3}	0.67	1.95
structure soln	Patterson	Patterson
absorption correct	XEMP	XABS
T_{max}, T_{min}	0.731, 0.603	0.681, 0.544

Geiger[24] and Finke[25] have demonstrated that cationic metal arene complexes can undergo simultaneous 2e reduction. These reductions are associated with an η^6-to-η^4 change in the hapticity of the arene (eq 4). This rearrangement is related to our results on $[\mathbf{1}]^{2+}$ insofar as both sets of compounds can be viewed as polyhedral clusters.[26] The results on the arene reduction are of further interest since they suggest an alternative structural possibility for the 50e clusters $[(arene)M]_3S_2^0$. In this alternative structure the closo M_3S_2 core is retained, but one arene adopts the η^4 geometry. One way this diene-closo isomer could be stabilized is by strengthening the M–M bonds relative to the M–L bonds. $[\mathbf{2}]^0$ may in fact adopt this structure.

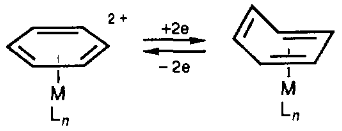

(4)

---

(14) Sappa, E.; Gambino, O.; Cetini, G. *J. Organomet. Chem.* **1972**, *35*, 375. Johnson, B. F. F.; Lewis, J.; Lodge, P. G.; Raithby, P. R.; Henrick, K.; McPartlin, M. *J. Chem. Soc., Chem. Commun.* **1979**, 719. Adams, R. D.; Babin, J. E. *Inorg. Chem.* **1986**, *25*, 4010.

(15) Related syntheses of M_3S_2 clusters, $[Pt(PR_3)_2]_3S_2^{2+}$: Chatt, J.; Mingos, D. M. P. *J. Chem. Soc. A* **1970**, 1243. Bushnell, G. W.; Dixon, K. R.; Ono, R.; Pidcock, A. *Can. J. Chem.* **1984**, *62*, 696. $[Pt(PR_3)_2]_2Rh(diene)S_2^+$: Briant, C. E.; Gilmour, D. I.; Luke, M. A.; Mingos, D. M. P. *J. Chem. Soc., Dalton Trans.* **1985**, 851. $H[Rh(diene)]_3S_2$: Arif, A. M.; Jones, R. A. *Polyhedron* **1988**, *7*, 561. $[Rh_3S_3Cl_2(PEt_3)_6]^+$: Galli, D.; Garlaschelli, L.; Chiani, G.; Fumagalli, A.; Martinengo, S.; Sironi, A. *J. Chem. Soc., Dalton Trans.* **1984**, 55.

(16) Greenwood, N. N.; Earnshaw, A. *Chemistry of the Elements*; Permagon Press: New York, **1984**; p 807. Jolly, W. L. *Modern Inorganic Chemistry*; McGraw-Hill: New York, 1984; p 198.

(17) Kim, T. D.; McNeese, T. J.; Rheingold, A. L. *Inorg. Chem.* **1988**, *27*, 2554 and references therein.

(18) Amarasekera, J.; Rauchfuss, T. B.; Wilson, S. R. *J. Chem. Soc., Chem. Commun.* **1989**, 14.

(19) Madach, T.; Vahrenkamp, H. *Chem. Ber.* **1981**, *114*, 505. Rives, A. R.; Xiao-Zang, Y.; Fenske, R. F. *Inorg. Chem.* **1982**, *21*, 2286.

(20) Zanello, P. *Coord. Chem. Rev.* **1988**, *83*, 199.

(21) Moran, M.; Cuadrado, I.; Masaguer, J. R.; Losada, J. *J. Chem. Soc., Dalton Trans.* **1988**, 833. Fenton, D. E.; Schroeder, R. R.; Lindvedt, R. L. *J. Am. Chem. Soc.* **1978**, *100*, 1931. Kini, A.; Mays, M.; Cowan D. *J. Chem. Soc., Chem. Commun.* **1985**, 286.

(22) Lockemeyer, J. R.; Rauchfuss, T. B.; Rheingold, A. L. Unpublished results.

(23) Bedard, R. L.; Dahl, L. F. *J. Am. Chem. Soc.* **1986**, *108*, 5933.

(24) Bowyer, W. J.; Geiger, W. E. *J. Am. Chem. Soc.* **1985**, *107*, 5657. Bowyer, W. J.; Merkert, J. W.; Geiger, W. E. *Organometallics* **1989**, *8*, 191. Bowyer, W. J.; Geiger, W. E. *J. Electroanal. Chem.* **1988**, *239*, 253.

(25) Finke, R. G.; Voegeli, R. H.; Laganis, E. D.; Boekelheide, V. *Organometallics* **1983**, *2*, 347.

(26) Mingos, D. M. P. *Acc. Chem. Res.* **1984**, *17*, 311.

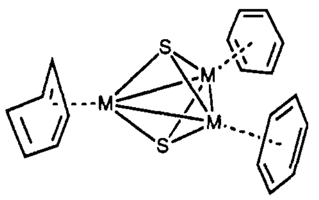

Experimental Section

Materials. RuCl$_3$·xH$_2$O was obtained as a loan from Johnson Matthey Inc. [(*p*-cymene)RuCl$_2$]$_2$,[27] [(*p*-cymene)OsCl$_2$]$_2$,[28] and (Me$_3$Si)$_2$S (Caution: STENCH!)[29] were prepared according to literature methods. Tetrahydrofuran was distilled from Na/K alloy. Diethyl ether was distilled from Na/benzophenone ketyl. Acetonitrile was distilled from CaH$_2$. Dichloromethane was distilled from P$_4$O$_{10}$. Nitromethane (Mallinckrodt, $\Lambda_e = 10^{-6}$ ohm^{-1} cm^2) for conductivity measurements was used as received. All solvents were distilled and stored under an atmosphere of dry, O$_2$ free nitrogen.

Methods. Elemental analyses were done by the University of Illinois Microanalytical Laboratory. ^{1}H and ^{13}C NMR spectra were obtained on a General Electric QE-300 spectrometer. UV–vis spectra were obtained on a Varian 2300 spectrophotometer. Conductivity measurements were taken at 26.5 °C using a YSI Scientific YSI-35 conductance meter. Positive ion FAB mass spectra were obtained at the mass spectrometry facility at the University of Illinois. Electrochemical experiments were done on a BAS-100 electrochemical analyzer. Cyclic voltammograms were measured on 10^{-3} M CH$_2$Cl$_2$ or CH$_3$CN solutions using 0.1 M Bu$_4$NPF$_6$ as supporting electrolyte, Pt working electrode, and a Pt counter electrode vs Ag/AgCl. Bulk electrolysis as CH$_3$CN solution used Bu$_4$NPF$_6$ as supporting electrolyte with a Pt working electrode at −1500 mV, using a Pt counter electrode vs Cp$_2$Fe/Cp$_2$Fe$^+$. All operations, unless otherwise stated, were performed under an atmosphere of nitrogen using standard Schlenk techniques.

[(*p*-Cymene)$_3$Ru$_3$S$_2$](PF$_6$)$_2$ from Aqueous Na$_2$S. In an open flask, a solution of Na$_2$S·9H$_2$O (0.261 g, 1.10 mmol) in 5 mL of H$_2$O was added dropwise to a solution of [(*p*-cymene)RuCl$_2$]$_2$ (0.500 g, 0.815 mmol) in 20 mL of H$_2$O. A rapid color change from orange to red-brown was accompanied by the formation of a small amount of brown precipitate. After 0.5 h, the mixture was filtered. To the filtrate was added solid KPF$_6$ (1.00 g, 5.43 mmol), and the resulting brown solid was filtered through Celite on a glass frit, washed with 2 × 10 mL of H$_2$O, and air dried 0.5 h. The precipitate was extracted from the Celite with CH$_2$Cl$_2$ until the washings were colorless, and the filtrate was dried over Na$_2$SO$_4$. The resulting red-brown CH$_2$Cl$_2$ solution was concentrated to a volume of about 10 mL. Hexanes were added until the solution became cloudy, and the solution was further concentrated in vacuo, affording a brown-black crystalline solid. The solid was filtered, washed with hexanes, and dried in vacuo to give 0.253 g (44%) of [**1**](PF$_6$)$_2$. FAB MS (^{102}Ru) 771 [(cymene)$_3$Ru$_3$S$_2$]$^+$; ^{1}H NMR (CD$_2$Cl$_2$) δ 5.80 (m, 12 H), 2.77 (sept, J = 3 Hz, 3 H), 2.45 (s, 9 H), 1.35 (d, J = 3 Hz, 18 H); UV–vis (CH$_2$Cl$_2$) $\lambda_{\max}$, nm (log ϵ) 485 (2.93), 386 (3.36), 336 (3.90). Anal. Calcd for C$_{30}$H$_{42}$F$_{12}$P$_2$Ru$_3$S$_2$: C, 33.99; H, 3.99; S, 6.05. Found: C, 33.95; H, 3.91; S, 5.99.

[(*p*-Cymene)$_3$Ru$_3$S$_2$](PF$_6$)$_2$ from Methanolic NaSH. To a stirred solution of [(*p*-cymene)RuCl$_2$]$_2$ (0.200 g, 0.326 mmol) in 10 mL of MeOH was added a solution of NaSH (0.366 g, 0.653 mmol) in 5 mL of MeOH. The resulting red-brown solution was stirred 1 h, and then solid KPF$_6$ (0.500 g, 2.71 mmol) was added. The solvent was stripped off in vacuo, and the solid was extracted into 10 mL of CH$_2$Cl$_2$. Crystallization by concentrating the solution, followed by addition of Et$_2$O produced a brown-black solid, which was dried in vacuo: yield 0.133 g, 58%. The ^{1}H NMR spectrum in CD$_2$Cl$_2$ was identical with that prepared as above.

[(*p*-Cymene)$_3$Ru$_3$S$_2$](PF$_6$)$_2$ Using (Me$_3$Si)$_2$S. Neat (Me$_3$Si)$_2$S (1.50 mL, 7.15 mmol) was slowly added to a stirred suspension of [(*p*-cymene)RuCl$_2$]$_2$ (3.00 g, 4.90 mmol) in 250 mL of warm THF. The solid dissolved to give a chocolate-brown solution, which quickly afforded a brown precipitate. The mixture was stirred 0.75 h, filtered, washed with THF (10 mL), and dried in vacuo overnight. The remaining portion of the experiment was performed in air. The dried microcrystalline solid was dissolved in 20 mL of H$_2$O, accompanied by some foaming. Solid KPF$_6$ (2.00 g, 10.9 mmol) was added to the clear aqueous solution, and the resulting brown precipitate was worked up as in the Na$_2$S reaction: yield 2.68 g (77%); conductivity (CH$_3$NO$_2$) 179 ohm^{-1} cm^2 mol^{-1}; IR (KI pellet) 3089 w, 3043 w, 2970 w, 2930 wsh, 1445 m, 1374 m, 1114 m, 861 vs, 840 s. Anal. Calcd for C$_{30}$H$_{42}$F$_{12}$P$_2$Ru$_3$S$_2$: C, 33.99; H, 3.99; S, 6.05. Found: C, 34.00; H, 3.92; S, 6.10.

Table III. Atomic Coordinates (×10^4) and Isotropic Thermal Parameters (Å^2 × 10^3) for [**1**](PF$_6$)$_2$

	x	y	z	U^a
Ru(1)	1009.9 (5)	1847.6 (5)	2498.8 (3)	35.5 (2)
Ru(2)	1349.9 (5)	−537.0 (5)	2133.7 (3)	35.9 (2)
Ru(3)	−1283.2 (5)	−643.2 (5)	2465.1 (3)	35.8 (2)
S(1)	773 (2)	334 (2)	3233.1 (8)	41.0 (6)
S(2)	−68 (2)	83 (2)	1494.8 (8)	40.1 (6)
P(1)	7128 (2)	3688 (2)	1113 (1)	64.0 (9)
P(2)	6439 (2)	3162 (2)	3930 (1)	68 (1)
C(1)	351 (7)	3502 (6)	2840 (4)	47 (3)
C(2)	1300 (7)	3613 (6)	3425 (4)	55 (3)
C(3)	2641 (7)	3711 (7)	3244 (4)	60 (3)
C(4)	3031 (6)	3706 (6)	2511 (4)	55 (3)
C(5)	2066 (6)	3592 (7)	1921 (4)	50 (3)
C(6)	715 (6)	3481 (6)	2099 (4)	50 (3)
C(7)	2536 (8)	3669 (8)	1142 (4)	70 (4)
C(8)	3319 (11)	5129 (9)	1081 (6)	119 (6)
C(9)	1379 (9)	2868 (9)	497 (4)	95 (5)
C(10)	887 (9)	3594 (8)	4210 (4)	80 (4)
C(11)	3544 (7)	−14 (7)	1853 (4)	50 (3)
C(12)	3375 (6)	−460 (7)	2525 (4)	52 (3)
C(13)	2318 (6)	−1743 (7)	2592 (4)	53 (3)
C(14)	1351 (7)	−2566 (7)	1945 (4)	61 (3)
C(15)	1518 (8)	−2106 (7)	1256 (4)	59 (3)
C(16)	2609 (7)	−864 (7)	1195 (4)	55 (3)
C(17)	2218 (8)	−2155 (10)	3344 (5)	90 (5)
C(18)	692 (8)	−3008 (9)	3498 (5)	86 (5)
C(19)	3191 (11)	−2563 (15)	3520 (8)	197 (11)
C(20)	2760 (10)	−358 (10)	471 (4)	89 (6)
C(21)	−2738 (7)	−1602 (7)	3319 (4)	55 (3)
C(22)	−2794 (6)	−2603 (7)	2718 (4)	59 (3)
C(23)	−3134 (6)	−2555 (7)	1971 (4)	59 (3)
C(24)	−3450 (6)	−1502 (7)	1814 (4)	51 (3)
C(25)	−3274 (6)	−448 (7)	2415 (4)	47 (3)
C(26)	−2914 (6)	−477 (7)	3153 (4)	51 (3)
C(27)	−2407 (9)	−1687 (10)	4115 (5)	90 (5)
C(28)	−1973 (14)	−375 (12)	4680 (5)	149 (10)
C(29)	−3710 (12)	−2825 (13)	4333 (7)	149 (9)
C(30)	−3852 (8)	−1469 (8)	1022 (4)	74 (4)
F(1)	8420 (8)	3765 (9)	693 (5)	182 (6)
F(2)	6161 (10)	2765 (8)	414 (5)	208 (6)
F(3)	5917 (7)	3653 (9)	1594 (4)	168 (6)
F(4)	8173 (7)	4629 (7)	1836 (4)	146 (4)
F(5)	7175 (11)	4955 (8)	860 (4)	195 (7)
F(6)	7135 (8)	2422 (6)	1380 (4)	140 (4)
F(7)	5486 (10)	3387 (13)	3443 (5)	260 (10)
F(8)	7735 (7)	4420 (6)	3851 (4)	178 (4)
F(9)	7340 (12)	2828 (11)	4457 (5)	239 (9)
F(10)	5208 (10)	1880 (8)	4052 (4)	252 (6)
F(11)	6152 (7)	3989 (7)	4633 (4)	161 (4)
F(12)	6739 (7)	2313 (6)	3233 (3)	137 (4)

[a] Equivalent isotropic U defined as one third of the trace of the orthogonalized $\mathbf{U}_{ij}$ tensor.

[(*p*-Cymene)$_3$Os$_3$S$_2$](PF$_6$)$_2$ [2](PF$_6$)$_2$. To a stirred solution of [(*p*-cymene)OsCl$_2$]$_2$ (0.150 g, 0.190 mmol) in 50 mL of THF was added neat (Me$_3$Si)$_2$S (53 μL, 0.253 mmol). The reaction mixture was refluxed for 24 h, during which time golden microcrystals of [**2**]Cl$_2$ formed. The solid was filtered off, washed with 2 × 2 mL THF, and dried in vacuo. The remainder of the experiment was performed in air and worked up as above to give the product as a reddish microcrystalline solid from CH$_2$Cl$_2$/hexanes: yield 85 mg (50%); ^{1}H NMR (CD$_2$Cl$_2$) δ 6.11 (br m, 4 H), 2.75 (sept, J = 3 Hz, 1 H), 2.61 (s, 3 H), 1.34 (d, J = 3 Hz, 6 H); UV–vis (CH$_2$Cl$_2$) $\lambda_{\max}$, nm (log ϵ) 500 (2.75), 413 (3.39), 344 (3.62), 298 (4.28), 277 (4.27). Anal. Calcd for C$_{30}$H$_{42}$F$_{12}$P$_2$Os$_3$S$_2$: C, 27.15; H, 3.19; S, 4.83. Found: C, 26.84; H, 3.13; S, 5.03.

(*p*-Cymene)$_3$Ru$_3$S$_2$ [1]^0. A solution of [**1**](PF$_6$)$_2$ (0.997 g, 0.941 mmol) in 10 mL of CH$_3$CN was transferred via cannula to a solution of Cp$_2$Co (0.356 g, 1.88 mmol) in 50 mL of CH$_3$CN. The solution immediately turned deep blue and was stirred for 0.75 h. The solvent was then removed in vacuo, and the remaining solid was dried in vacuo for 1 h. The resulting solid was extracted into 10 mL of THF, filtered to remove Cp$_2$Co(PF$_6$), and stripped in vacuo to give a blue-black microcrystalline

---

(27) Bennett, M. A.; Smith, A. K. *J. Chem. Soc., Dalton Trans.* **1974**, 233. Bennett, M. A.; Huang, T.-N.; Matheson, T. W.; Smith, A. K. *Inorg. Synth.* **1982**, *21*, 74.

(28) Cabeza, J. A.; Maitlis, P. M. *J. Chem. Soc., Dalton Trans.* **1985**, 573.

(29) Armitage, D. A.; Clark, M. J.; Sinden, A. W.; Wingfield, J. N.; Abel, E. W.; Louis, E. J. *Inorg. Synth.* **1974**, *15*, 207.

Table IV. Atomic Coordinates ($\times 10^4$) and Isotropic Thermal Parameters ($Å^2 \times 10^3$) for [**1**]^0

	x	*y*	*z*	*U*
Ru(1)	4312.4 (6)	2272.7 (5)	3835.1 (3)	39.4 (2)[a]
Ru(2)	3826.9 (6)	2742.3 (5)	2056.2 (3)	38.6 (2)[a]
Ru(3)	3681.7 (6)	76.0 (5)	2407.5 (3)	41.5 (2)[a]
S(1)	2507 (2)	1680 (2)	3215 (1)	43.7 (5)[a]
S(2)	5450 (2)	980 (2)	2822 (1)	43.4 (5)[a]
C(1)	4050 (9)	1984 (8)	5292 (4)	59 (3)[a]
C(2)	3220 (9)	3224 (8)	4935 (5)	64 (3)[a]
C(3)	3822 (9)	4186 (7)	4340 (5)	62 (3)[a]
C(4)	5236 (9)	5934 (7)	4105 (5)	59 (3)[a]
C(5)	6054 (9)	2698 (8)	4474 (5)	61 (3)[a]
C(6)	5427 (9)	1716 (7)	5063 (4)	60 (3)[a]
C(7)	7671 (12)	2319 (14)	4193 (9)	117 (6)[a]
C(8)	8511 (25)	2016 (25)	4981 (16)	141 (9)
C(8′)	8243 (28)	1028 (29)	4519 (18)	73 (10)
C(9)	8055 (13)	3177 (13)	3389 (9)	128 (7)[a]
C(10)	1719 (11)	3445 (11)	5155 (7)	99 (5)[a]
C(11)	4802 (9)	4475 (7)	1472 (5)	66 (3)[a]
C(12)	3399 (8)	4995 (6)	1727 (5)	57 (3)[a]
C(13)	2322 (8)	4568 (7)	1399 (4)	55 (3)[a]
C(14)	2634 (9)	3580 (7)	850 (4)	59 (3)[a]
C(15)	4014 (10)	3109 (8)	585 (5)	69 (3)[a]
C(16)	5110 (9)	3557 (8)	886 (5)	71 (3)[a]
C(17)	838 (8)	5051 (8)	1641 (6)	67 (3)[a]
C(18)	299 (12)	6271 (12)	921 (8)	116 (6)[a]
C(19)	609 (11)	5401 (10)	2564 (7)	62 (5)[a]
C(20)	6586 (11)	3005 (11)	653 (7)	127 (5)[a]
C(21)	2000 (11)	−693 (11)	1928 (9)	107 (6)[a]
C(22)	2919 (13)	−339 (10)	1223 (7)	101 (5)[a]
C(23)	4293 (11)	−881 (9)	1245 (5)	79 (4)[a]
C(24)	4872 (9)	−1784 (7)	2004 (6)	65 (3)[a]
C(25)	3978 (10)	−2143 (7)	2722 (5)	66 (3)[a]
C(26)	2575 (10)	−1597 (8)	2683 (7)	82 (4)[a]
C(27)	474 (18)	−69 (24)	1901 (18)	214 (14)[a]
C(28)	−2 (31)	667 (39)	1286 (32)	686 (33)[a]
C(29)	−299 (20)	−310 (30)	2701 (21)	341 (23)[a]
C(30)	6380 (11)	−2316 (11)	2100 (10)	121 (7)[a]

[a] Equivalent isotropic *U* defined as one third of the trace of the orthogonalized $\mathbf{U}_{ij}$ tensor.

solid: yield 0.660 g (92%); ^{1}H NMR (C_6D_6) δ 5.62 (m, 4 H), 5.13 (m, 4 H), 5.01 (m, 4 H), 2.35 (m, 3 H), 1.98 (s, 3 H), 1.76 (s, 6 H), 1.23 (d, 6 H), 1.13 (d, 12 H); ^{13}C[^{1}H] NMR (C_6D_6) δ 19.2, 20.9, 23.6, 24.2, 32.7, 33.5, 76.0, 78.2, 80.7, 83.2, 89.1, 99.5, 106.7, 108.7; UV–vis (CH_3CN) λ_{max}, nm 576, 392. Anal. Calcd for $C_{30}H_{42}Ru_3S_2$: C, 46.80; H, 5.50. Found: C, 46.67; H, 5.50.

Reaction of [1]^0 with $HOSO_2CF_3$, Formation of [1](OTf)$_2$. To a solution of [**1**]^0 (0.105 g, 0.136 mmol) in 10 mL of Et_2O was added triflic acid (12 μL, 0.136 mmol). The immediate formation of a burnt orange precipitate was accompanied by the evolution of a gas. The solid was filtered off, washed with Et_2O, and dried in vacuo to give a 58-mg product. The remaining deep blue filtrate was treated with another equivalent of HOTf, producing the same results and a yield of an additional 50-mg product. At this point no blue color remained in the mother liquor: yield 108 mg, 74% based on [**1**](OTf)$_2$. ^{1}H NMR (CD_2Cl_2) δ 5.90 (m, 12 H), 2.78 (sept, 3 H), 2.46 (s, 9 H), 1.35 (d, 18 H); UV–vis (CH_2Cl_2) λ_{max}, nm 485, 386, 336. Anal. Calcd for $C_{32}H_{42}F_6O_6Ru_3S_4$: C, 35.98; H, 3.96; F, 10.67; S, 12.10. Found: C, 36.10; H, 4.08; F, 10.55; S, 11.94.

Crystallography. $C_{30}H_{42}F_{12}P_2Ru_3S_2$, [**1**]($PF_6$)$_2$. Crystals of [**1**]($PF_6$)$_2$ were grown by diffusion of Et_2O into a CH_2Cl_2 solution of the cluster. A brown plate of crystal dimensions 0.07 × 0.25 × 0.42 mm was mounted on a glass fiber. Crystal, data collection, and refinement parameters are listed in Table II. Atomic coordinates and isotropic thermal parameters are listed in Table III.

$C_{30}H_{42}Ru_3S_2$, [**1**]^0. Crystals suitable for X-ray diffraction study were grown by vapor diffusion of hexanes into a toluene solution of the cluster. A black crystal of dimensions 0.35 × 0.30 × 0.40 mm was mounted on a glass fiber. Crystal, data collection, and refinement parameters are listed in Table II. Atomic coordinates and thermal parameters are listed in Table IV. Isopropyl groups associated with Ru(1) and Ru(3) exhibit some disorder that was successfully modeled for Ru(1) with the location of an alternate C(8) atom (C(8′)). Attempts to model disorder for C(27) to C(29) proved unsuccessful. All computations used SHELXTL (5.1) software (G. Sheldrick, Nicolet XRD, Madison, WI).

Acknowledgment. This research was supported by the National Science Foundation. Acknowledgment is also made to the donors of the Petroleum Research Fund, administered by the American Chemical Society. Johnson Matthey is thanked for the loan of ruthenium trichloride.

Supplementary Material Available: Tables of atomic coordinates, bond lengths and angles, anisotropic thermal parameters, and hydrogen atom coordinates (12 pages); tables of observed and calculated structure factors (57 pages). Ordering information is given on any current masthead page.